

Electronic Supplementary Information

Molecular Hot Spots in Surface-Enhanced Raman Scattering

Ming Li^{b,c,#}, Scott K. Cushing^{d,#}, Guangwen Zhou^e, and Nianqiang Wu^{a,c,*}

^aDepartment of Chemical Engineering, University of Massachusetts Amherst, Amherst, MA 01003-9303, United States

^bSchool of Materials Science and Engineering, Central South University, Changsha, Hunan 410083, China

^cDepartment of Mechanical and Aerospace Engineering, West Virginia University, Morgantown, WV 26506-6106, USA

^dChemistry and Chemical Engineering, California Institute of Technology, Pasadena CA 91125

^eDepartment of Mechanical Engineering and Multidisciplinary Program in Materials Science and Engineering, State University of New York, Binghamton, New York 13902, USA

[#]These authors contributed equally.

*To whom the correspondence should be addressed. Fax: +1-413-545-1647, E-mail: nianqiangwu@umass.edu

S1. Discrete Dipole Approximation (DDA) and Effective Dielectric Constant. The dielectric function describes from a macroscopic point of view the optical properties of a metal. In the visible spectrum, the dielectric properties of Au are described by both a Drude term describing collisions and a term describing the interband transitions.

$$\varepsilon = 1 - \frac{\omega_p^2}{\omega^2 - i\omega\gamma(R)} + X^{ib} \quad (S1)$$

where ω_p

$$\omega_p = \sqrt{\frac{n_e \cdot e^2}{m_e \cdot \varepsilon_0}} \quad (S2)$$

Since the dielectric function shows the response of the oscillation of the free electrons to the oscillating electromagnetic field, the term $\gamma(R)$ can be seen as the dampening. During LSPR, when the electrons have a collision they become out of phase with the other electrons in oscillation, causing the width of the resonance to broaden.¹ As the particle's size becomes less than the electron mean free path in the metal (radius < 5 nm) or when adsorbed surface states are taken into account, the function $\gamma(R)$ must be modified from its bulk value.

$$\gamma(R) = \gamma_0 + \frac{A \cdot v_f}{R} \quad (S3)$$

where γ_0 is the bulk value, A is a constant determined by the surface interface dampening, or (CID), v_f is the Fermi velocity and R is the radius of the particle.² The dielectric function is further modified as the radius approaches 1 nm because the density of states and Fermi velocity are changed due to quantum confinement.¹ However, these effects were not included since they did not produce significant modification at the size of particle investigated. The value of A depends on the adsorbed surface states present. Qualitatively speaking, if the adsorbed molecule creates a band in the density of states close to the Fermi level of Au, electrons can transfer into the created band under photoexcitation, backscatter, and then transfer back into the Fermi level. When under SPR excitation, these electrons can return out of phase, broadening or destroying the SPR peak. The size and CID dependent dielectric function was determined by the method used in Ref 1. The bulk constants were determined by using the data from Palik.³ The values for the constant A were determined by using DFT data⁴ to determine the local DOS when a molecule is absorbed, then comparing the value for the width and energy with the values from the graphs given in Ref 2. The dielectric constant was first checked using Mie theory to see if it produced a reasonable approximation of the experimental data. For the 3nm MBA coated nanoparticles this confirmed a value of $A=7$ was correct, while for the MPA coated nanoparticles a value of $A=1$ with one electron donated per MPA described the data.

Once the dielectric function was modified for the case of 3 nm Au NPs (where CID and distance dependent terms dominate), the Discrete Dipole Approximation was used to model

the coupled spheres. The open source DDSCAT code was used in all simulations.⁵ The outer 0.75 nm was represented by the CID dampened dielectric function (determined by the DFT data in Ref 4). The inner shell ($R_{\text{inner}} = R_{\text{total}} - 0.75\text{nm}$) was taken to be a size adjusted, but not chemically dampened, dielectric function. The interdipole distance in the model determines the distance between the two Au spheres. Each model used greater than 10^5 dipoles for convergence, which resulted in the following separation distances:

3 nm = 0.225 nm separation

15 nm = 0.25 nm separation

80 nm = 0.5 nm separation

The incident electromagnetic field was polarized along the axis joining the core shell particles, and the total $|E|^2$ field magnitude was output in the XZ plane.

References:

- 1 L. B. Scaffardi, N. Pellegrini and O. Sanctis, J. O. Tocho¹, *Nanotechnology*, 2005, **16**, 158-163.
- 2 A. Pinchuk and U. Kreibitz, *New J. Phys.*, 2003, **5**, 151.1-151.15.
- 3 E. D. Palik, *Handbook of optical constants of solids*; Academic Press: Boston, 1985.
- 4 Y. Li, G. Galli and F. Gygi, *ACS Nano*, 2008, **2**, 1896-1902.
- 5 B.T. Draine and P.J. Flatau, *J. Opt. Soc. Am. A*, 1994, **11**, 1491-1499.

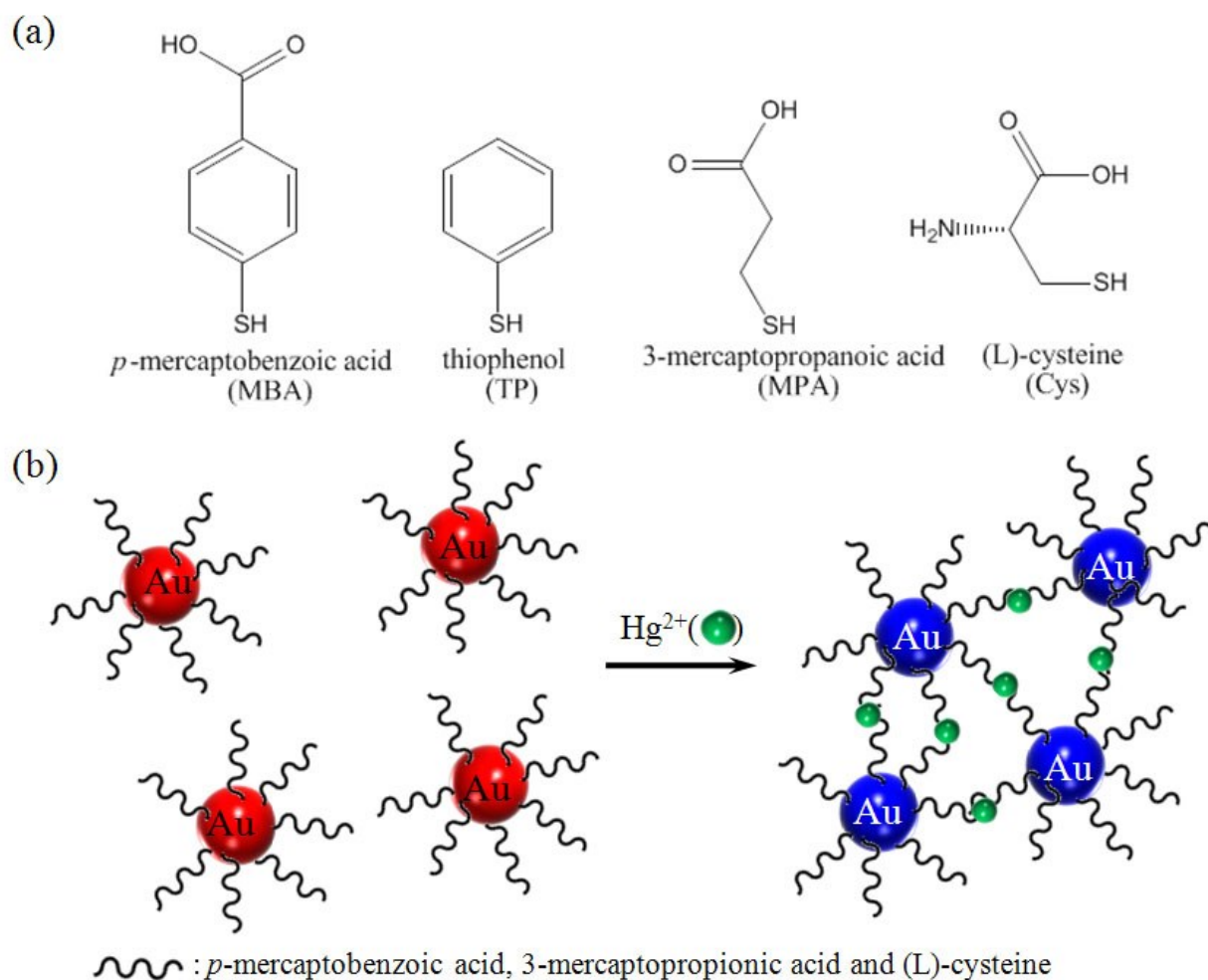


Figure S1. (a) Molecular structures of the ligands used, and (b) the schematic illustration of the “hot spot” formed by coordination chemistry between Hg^{2+} and carboxylic group.

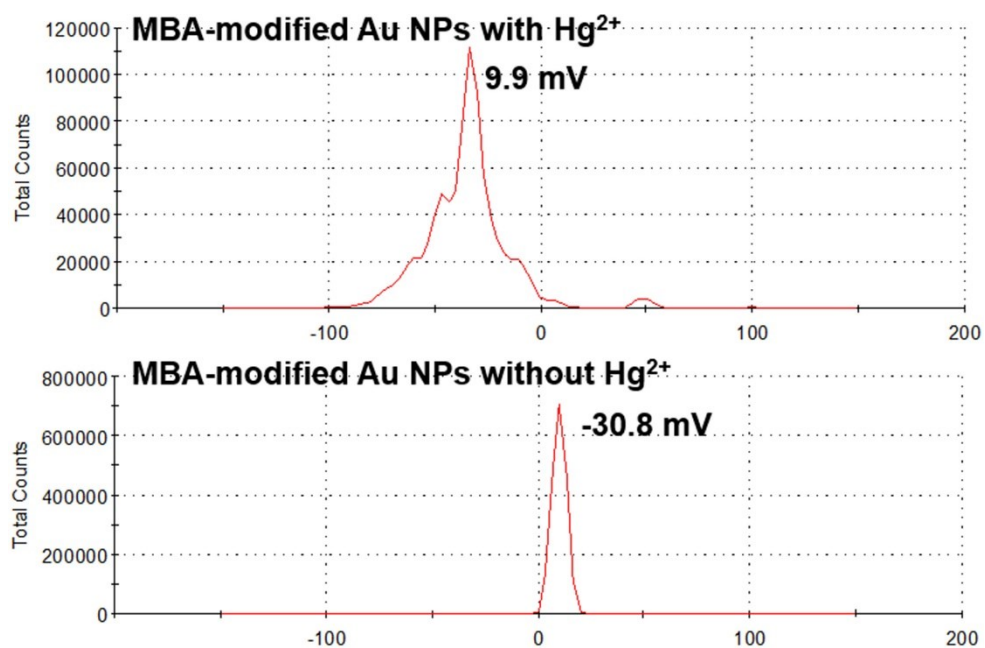


Figure S2. Zeta potential of MBA-modified Au NPs (15 nm) before and after addition of 5 mM Hg²⁺. The zeta potential shifts to +9.9 mV from -30.8 mV after the addition of 5 mM Hg²⁺.

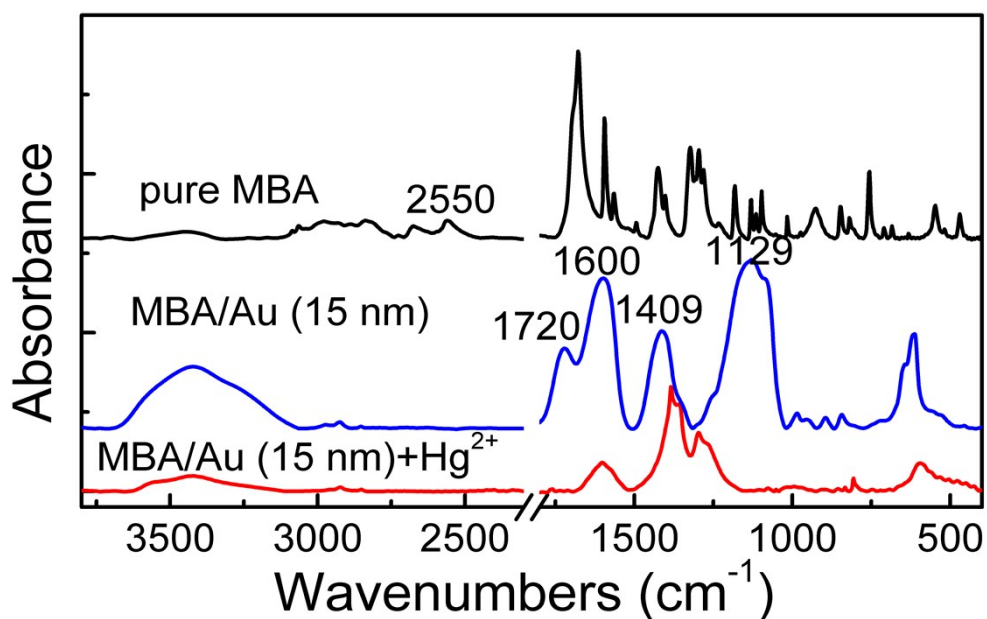


Figure S3. FTIR spectra of MBA, the MBA-functionalized Au nanoparticles (15 nm) and the Hg²⁺-linked Au aggregates. FTIR spectra show the disappearance of characteristic S-H peak at 2550 cm⁻¹ after chemi-adsorption of MBA on the Au nanoparticles, indicating the covalent binding of MBA to the Au nanoparticles. The disappearance of characteristic C=O peaks at 1720 cm⁻¹ in the FTIR spectrum of the Au aggregates after Hg²⁺ addition, confirming the formation of the Au-MBA-Hg²⁺-MBA-Au complex.

Table S1. Vibration mode assignment⁶ of FTIR peaks

of pure MBA and MBA on the 15 nm sized Au nanoparticle surface

Peak position (cm ⁻¹)	Assignment
3100-3600	O-H stretching
2550 and 2680	S-H stretching
1720 or 1670	C=O stretching
1600 and 1409	ring stretching
1129	C-O stretching

Disappearance of the peak at 2550 cm⁻¹ and the appearance of the peak at 1720 cm⁻¹ in the spectra of the MBA-modified Au nanoparticles have provided the direct evidence of covalent binding of MBA to the Au nanoparticle surface. After Hg²⁺ addition, disappearance of the peak at 1720 cm⁻¹ indicates that the carboxylic group coordinately binds to Hg²⁺, forming the Au-MBA-Hg²⁺-MBA-Au complex, which has resulted in the aggregation of Au nanoparticles.

Reference:

6 G. Socrates, *Infrared and Raman Characteristic Group Frequencies, Tables and Charts*, 3rd ed.; John Wiley & Sons, Ltd.: New York, 2001.

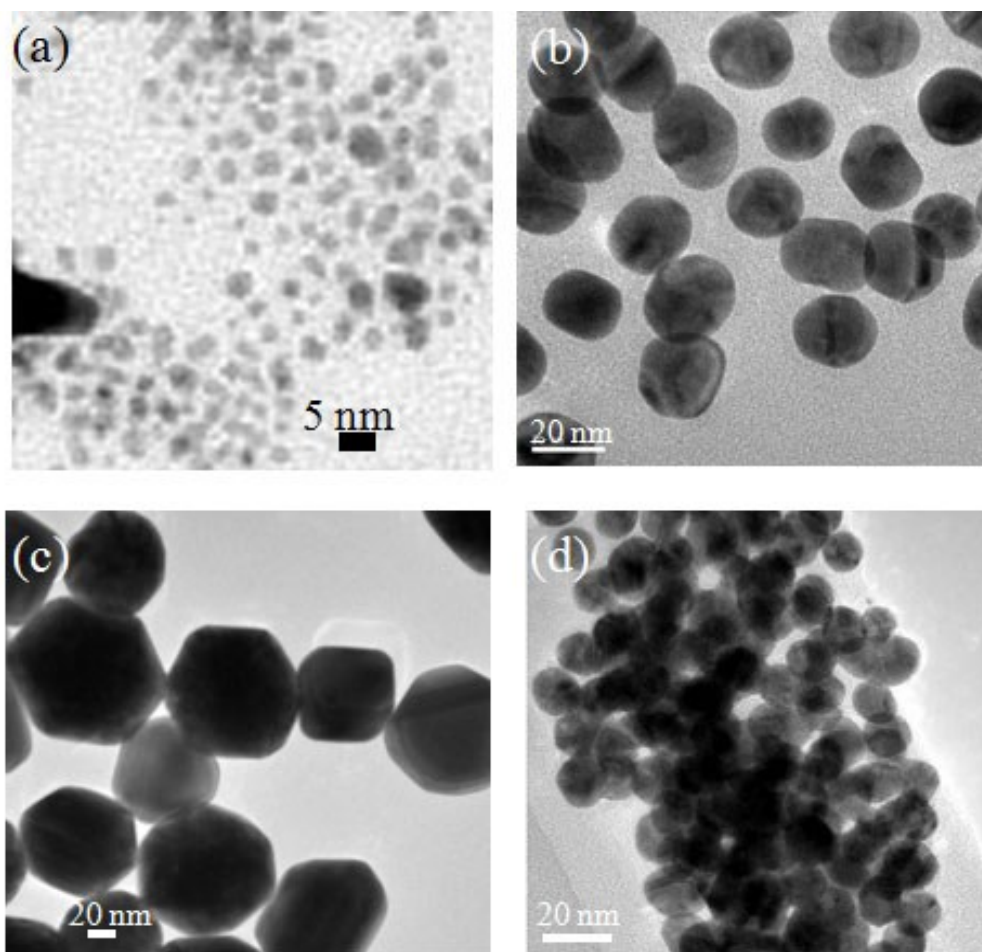


Figure S4. TEM images of (a) 3 nm, (b) 15 nm and (c) 80 nm sized Au nanoparticles functionalized with MBA before the addition of Hg^{2+} ; and (d) MBA-functionalized 15 nm sized Au nanoparticles in the presence of 5 mM Hg^{2+} .

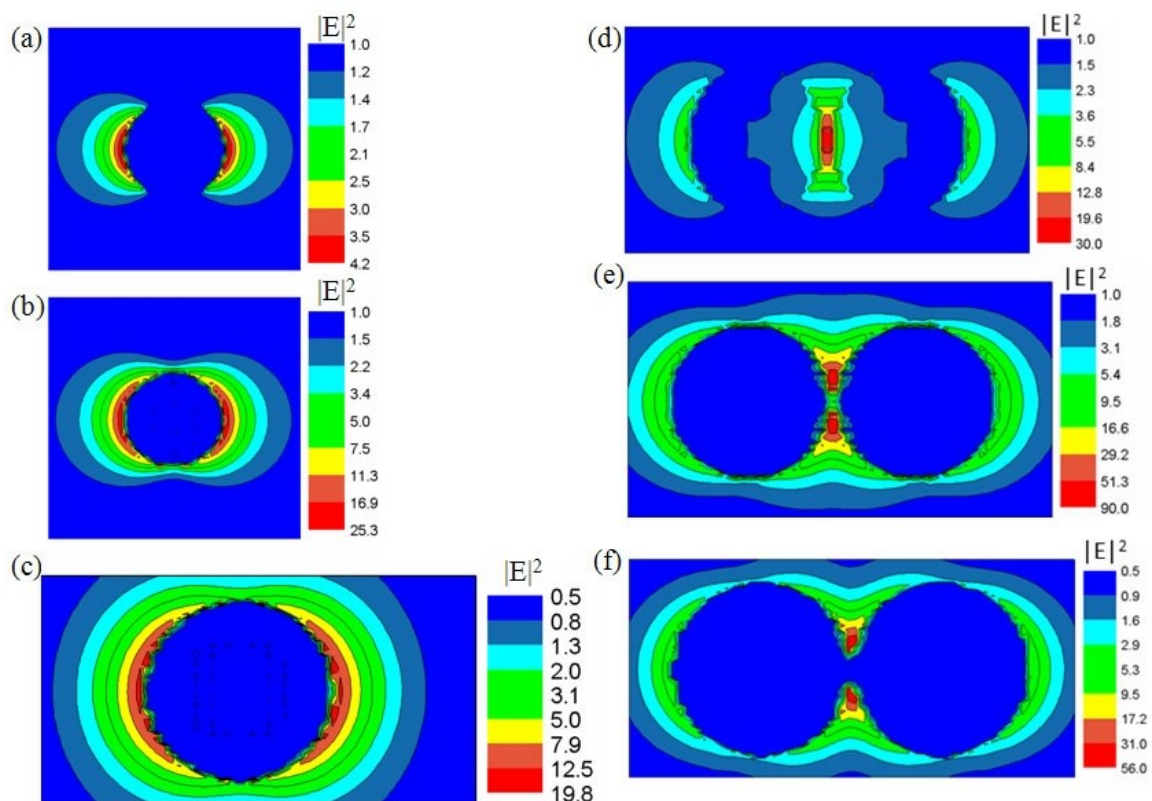


Figure S5. Magnitude of local electromagnetic field squared ($|E|^2$) surrounding single Au nanoparticle: (a) 3 nm, (b) 15 nm, and (c) 80 nm Au nanoparticles with an MBA fitted effective dielectric constant outerlayer. Incident light wavelength was 532 nm and linearly polarized along nanoparticle axis. Magnitude of local electromagnetic field squared ($|E|^2$) surrounding two adjacent Au nanoparticles: (d) 3 nm, (e) 15 nm, and (f) 80 nm Au nanoparticle dimer with an MBA fitted effective dielectric constant outerlayer. Incident light wavelength was 532 nm and linearly polarized along nanoparticle axis.

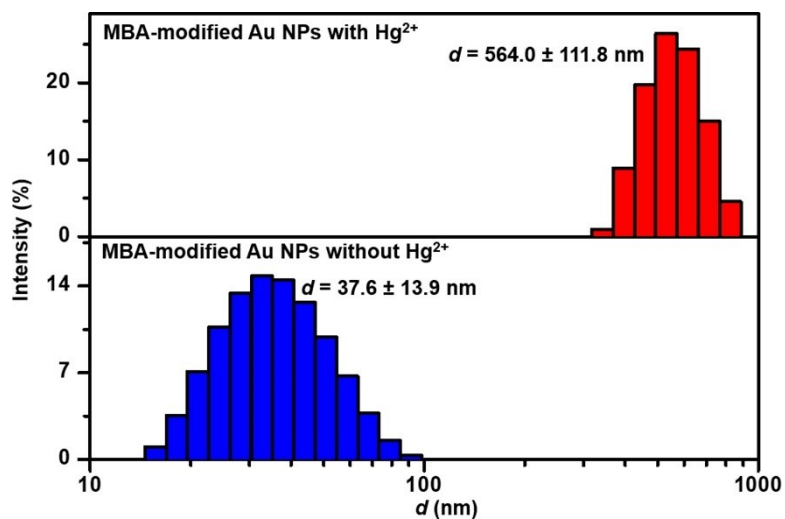


Figure S6. Hydrodynamic sizes of MBA-modified Au NPs (15 nm in diameter) before and after addition of 5 mM Hg²⁺. The addition of 5 mM Hg²⁺ to the suspension of MBA-modified Au NPs obviously increases the hydrodynamic size to 564.0 ± 111.8 nm from 37.6 ± 13.9 nm, indicating the induced aggregation or chelation of Hg²⁺ with the carboxyl group.

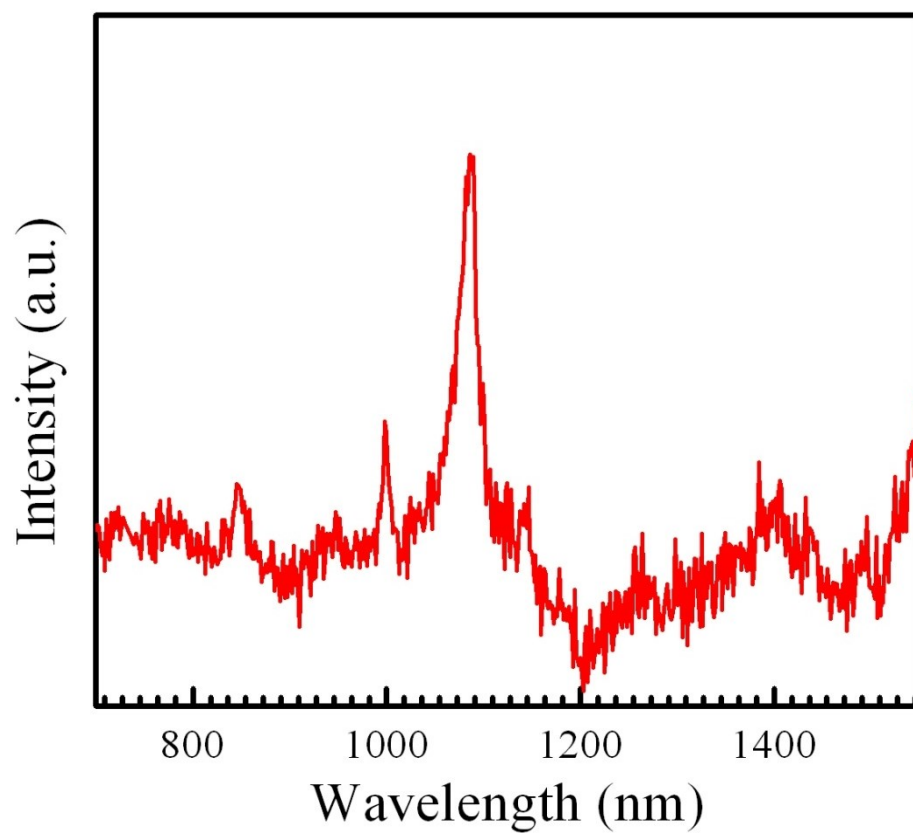


Figure S7. SERS spectrum of thiophenol immobilized on the 3 nm Au nanoparticles.

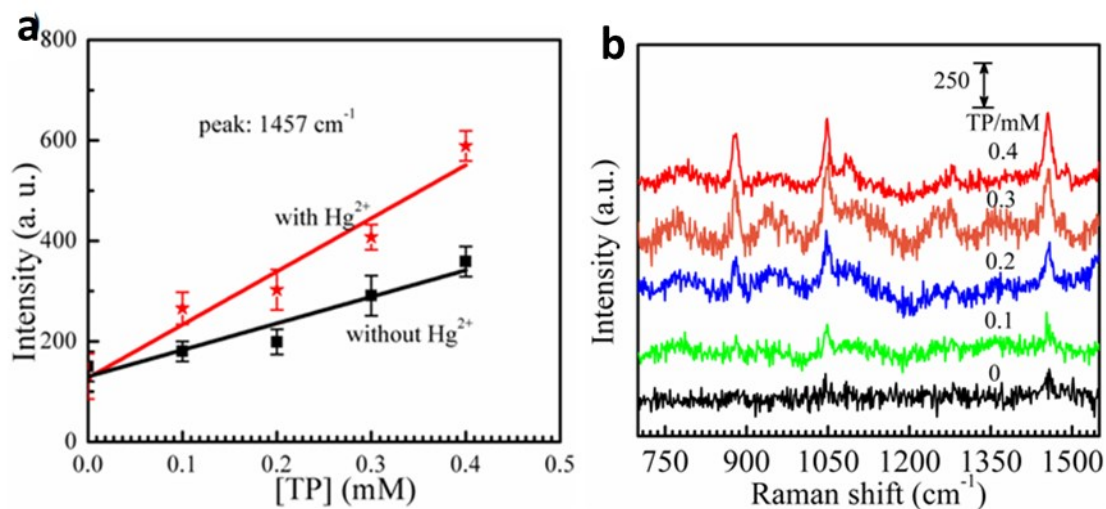


Figure S8. Enhancement of linear MPA SERS signal at a constant MPA concentration for 3 nm particles. (a) Plot of the 1457 cm⁻¹ peak intensity (from MPA) as a function of the TP concentration at 0.1 mM concentration of MPA in the absence and presence of 5 mM Hg²⁺; and (b) SERS spectra of TP/MPA co-immobilized on 3 nm Au nanoparticles in the absence and presence of Hg²⁺; (6 nM 3 nm Au NPs, pH=6.3). The laser power: 0.017 mW, and the acquisition time: 10 s.

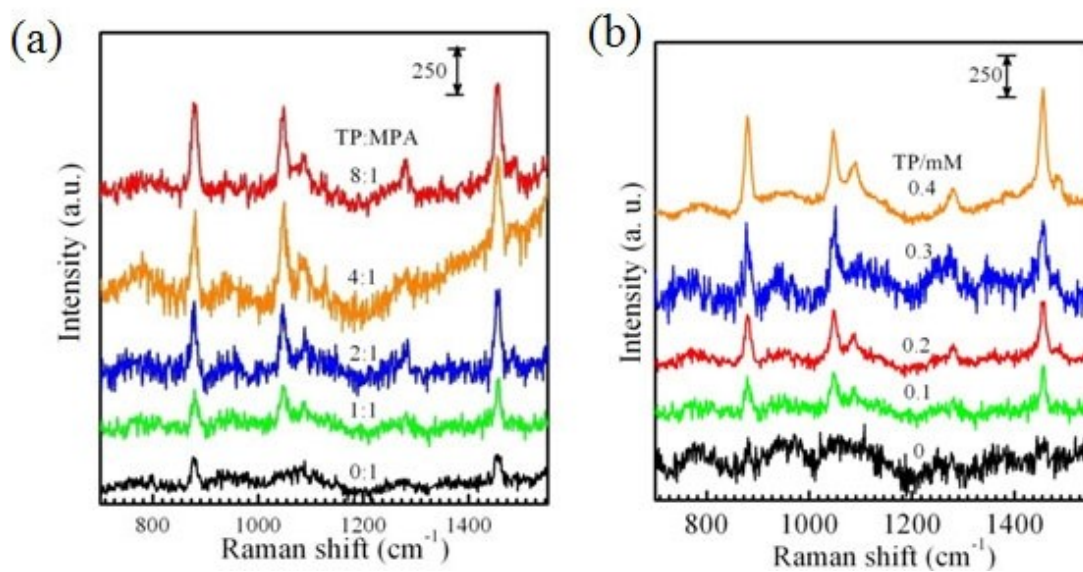


Figure S9. SERS spectra of the mixture of TP and MPA immobilized on the 3 nm Au nanoparticles in the presence of 5 mM Hg^{2+} for (a) the TP/MPA mixture at different TP/MPA ratios, and (b) the TP/MPA mixture at different TP concentrations.

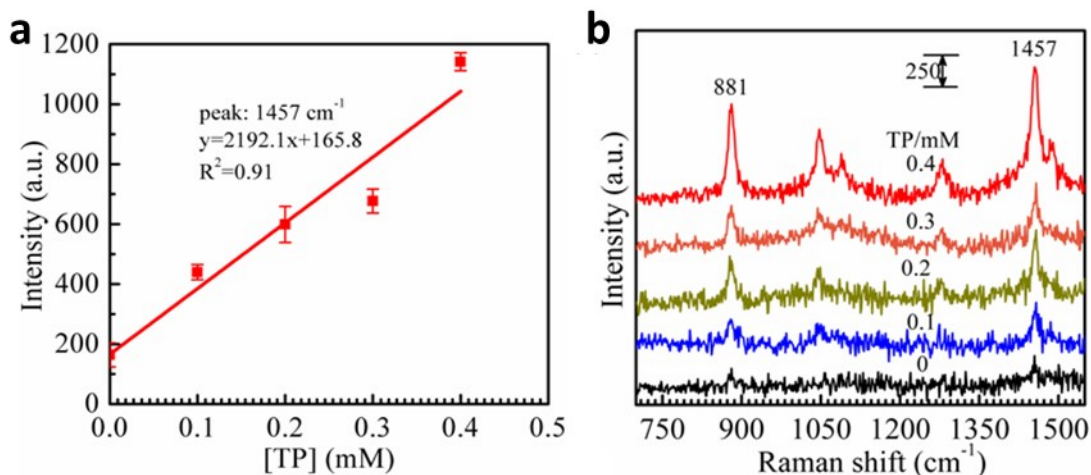


Figure S10. Enhancement of linear MPA SERS signal at a constant MPA concentration for 15 nm particles. (a) Plot of the SERS peak intensity at 1457 cm⁻¹ (from MPA) with an increase in the TP concentration at a constant concentration of MPA; and (b) SERS spectra of TP/MPA co-modified Au nanoparticles (6 nM 15 nm Au NPs, 0.1 mM MPA, 5 mM Hg²⁺ and pH=6.3). The laser power: 0.017 mW, and the acquisition time: 10 s.

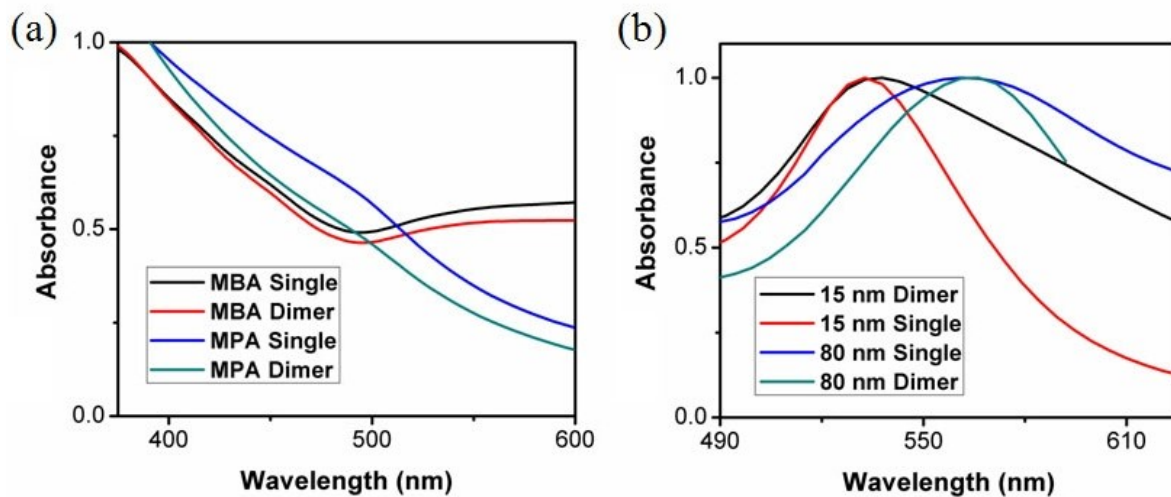


Figure S11. Discrete dipole approximation (DDA) simulated absorption spectra using a 0.75 nm layer for the Mie theory fitted dielectric constant for (a) single or dimer 3-nm Au nanoparticles coated with MBA and MPA, and (b) single or dimer Au nanoparticles coated with MBA (two different sizes are considered: 15 nm and 80 nm).

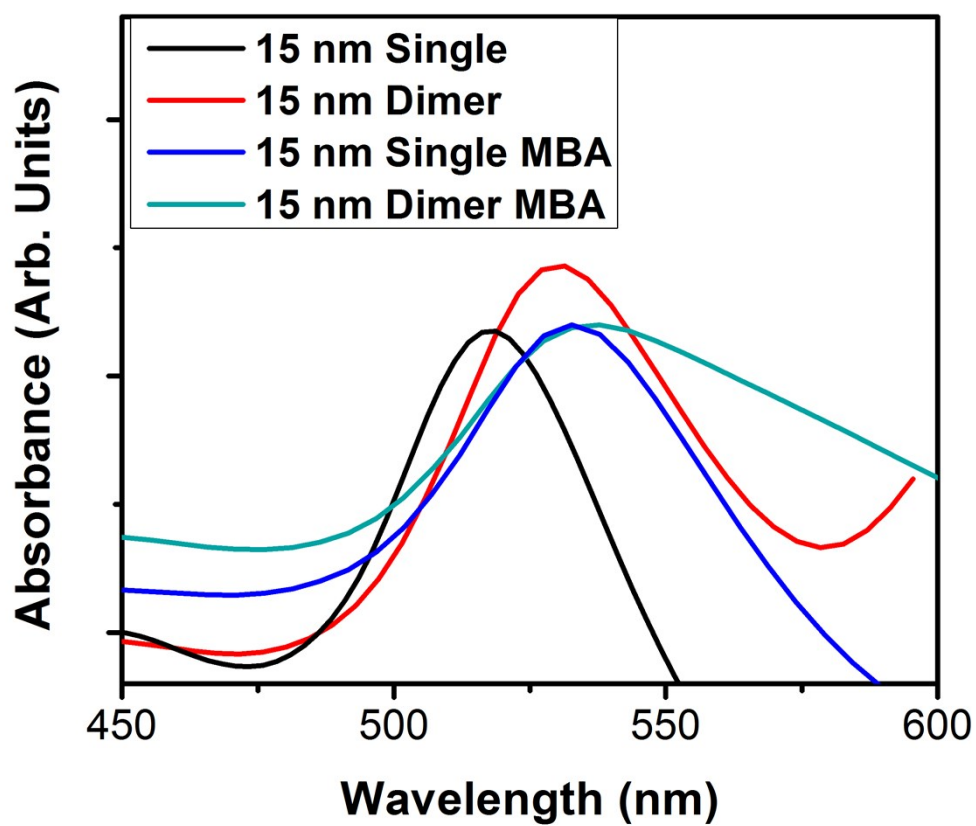


Figure S12. Discrete dipole approximation (DDA) simulated absorption spectra showing the difference in absorption with and without the CID MBA model. The peak broadening and small redshift seen in experiment is only replicated by the CID model.